PAPER *Special Issue on Microwave and Millimeter Wave Technology*

Investigation of RoF Link Noise Influence in Ubiquitous Antenna System

Shutai OKAMURA[†a)], ***Student Member***, **Minoru OKADA**[††],
Katsutoshi TSUKAMOTO[†], ***Regular Members***, *and* **Shozo KOMAKI**[†], ***Fellow***

SUMMARY This paper focuses on the investigation of RoF link noise influence in an ubiquitous antenna system, which is composed of multiple radio base stations (RBSs) deployed over the service area, central control station (CCS) and radio-on-fiber (RoF) link that connects RBSs to the CCS. The ubiquitous antenna system is capable of receiving multiple mobile terminals simultaneously operating at the same frequency channel by making effective use of joint detection. However, in the ubiquitous antenna system, since signals are transmitted from RBSs to CCS via the RoF link, the noise generated at the RoF link, such as relative intensity noise, inter modulation distortion, optical shot noise and thermal noise, may become dominant factors degrading the performance. The performance evaluations considering optical link noise is given by computer simulations. Computer simulation results show that more than 19 dB of RoF link E_b/N_0 is required for achieving sufficient performance.

key words: *ubiquitous antenna system, radio-on-fiber, optical link noise, joint detection, wireless LAN*

1. Introduction

The demand for high-speed and high-quality transmission in wireless communication environment has been increasing rapidly in recent years. The broadband wireless local area network (LAN) standards, such as IEEE 802.11a (US), HIPERLAN/2 (EU) and MMAC (Japan), provide information data rate of up to 54 Mbits/s by the use of coded orthogonal frequency division multiplex (COFDM) [1], [2]. However, there are disadvantages in those systems as follows; the bandwidth assigned to those systems is not sufficient for satisfying above demand, the low effective throughput, the gap in data transfer rate between wired and wireless communications and so on.

In order to realize higher-speed and higher-quality transmission, multiple-input multiple-output (MIMO) systems are widely studied [3]–[7]. In MIMO systems, multiple transmit antennas (or users) transmit different signals simultaneously at the same frequency channel, and the receiver detects the multiple signals by means of a spatial signal processing based on the signals received by the spatially deployed multiple antennas. Consequently, the system capacity is increased in terms of maximum transfer rate when multiple transmit antennas are set up in one user, or total number of users. The system, however, requires the independence of channel response between all mobile terminals (MTs) and RBSs in order to operate the MIMO system effectively. Hence, the capacity of the system is degraded because of the correlation between antenna elements when the MIMO system is realized by the use of the RBS which equips centralized multiple antenna elements.

On the other hand, ubiquitous antenna systems based on radio-on-fiber (RoF) technology have been proposed for next generation mobile radio communication networks [8]–[13]. Microcellular radio base stations (RBS) deployed over the service area are connected to a central control station (CCS) by optical fibers and radio signals are transmitted over an optical fiber link among RBSs and CCS with their original radio frequency (RF) signal format kept. In such a system, each RBS consist of simple optical-to-electrical (O/E) and/or electrical-to-optical (E/O) conversion devices. No other radio signal processing equipment such as modulator, demodulator and so on is installed at the RBS. On the other hand, all the modulation/demodulation functions, any other radio signal processors and controllers are installed at the CCS. Such concentrated implementation of these complicated functions provides a much simplified and cost-effective radio access network, and makes it easy to apply more sophisticated signal processing algorithms such as co-channel interference cancellation and multi-user detection. Furthermore, such a system are very flexible to the modification of radio signal formats or the opening of new radio services. Therefore we can share the system with various type of radio services. Consequently, the ubiquitous antenna system is considered as one of hopeful candidates for heterogeneous radio access networks including wireless LAN, fourth generation mobile communication systems, intelligent transport systems (ITS) and broadband wireless access (BWA).

The ubiquitous antenna system is considered as one of the MIMO systems. We have previously proposed the ubiquitous antenna system which can per-

Manuscript received November 29, 2002.
Manuscript revised March 31, 2003.

[†]The authors are with the Department of Communications Engineering, Faculty of Engineering, Osaka University, Suita-shi, 565-0871 Japan.
[††]The author is with the Graduate School of Information Science, Nara Institute of Science and Technology, Ikoma-shi, 630-0101 Japan.
a) E-mail: okamura@roms.comm.eng.osaka-u.ac.jp

form spatial diversity to maximize received signal to interference and noise ratio (SINR) [14]–[17]. In the proposed ubiquitous antenna system, the independent channels are easily obtained since multiple RoF-connected RBSs are deployed over the service area. The CCS performs the spatial signal processing by using the signals propagated via such independent channels same as the MIMO systems in order to detect the collided signals simultaneously received at the same frequency channel. As a result, the system can realize the space division multiple access (SDMA) equivalently, and its capacity can be remarkably improved.

In [17], we have also proposed a new type of COFDM based ubiquitous antenna system which employs minimum mean square error diversity combiner (MMSE-DC) based joint detector with mean square error (MSE) normalization, and investigated the uplink system performance under the condition of 5 GHz wireless LAN standard with considerations of multipath Rayleigh fading and RoF link propagation delay. It has been shown that the proposed ubiquitous antenna system achieves 3.6 times and 18% higher frequency utilization efficiency compared with single omniantenna system without performing the joint detection and the centralized antenna system which equips adaptive array antenna at a RBS [18], respectively.

In these previous works, we assumed relative high quality of a RoF link and ignored the performance degradation in optical link caused by relative intensity noise (RIN), non-linear distortion, optical shot noise and thermal noise. However, it has been shown that the noises generated at the RoF link become dominate factors degrading the performance of the system [11]–[13]. Therefore, we have investigated that how much impact the noises affect on the performance of the joint detection based on the ubiquitous antenna system [19].

This paper provides the performance investigations with considering optical link noise and estimation of the required optical link signal-to-noise ratio (SNR) for achieving higher performance compared with the other systems The rest of this paper is organized as follows. Section 2 illustrates the proposed ubiquitous antenna based wireless LAN system. Then, in Sect. 3, we analyze the system performance with considering the optical link noise. Computer simulations show superiority of the proposed system in the characteristics of received SINR and frequency utilization efficiency. Finally, concluding remark is given in Sect. 4.

2. Ubiquitous Antenna for Broadband Wireless LAN System

2.1 General Description

A configuration of the proposed ubiquitous antenna based wireless LAN system is illustrated in Fig. 1. The proposed system is composed of multiple RBSs, the

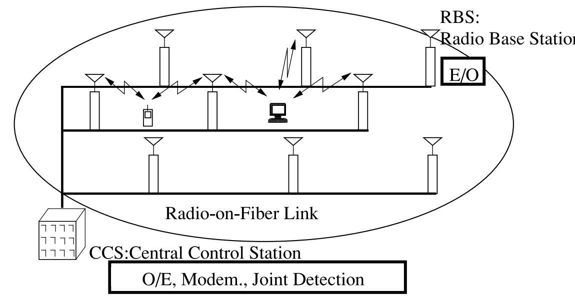

Fig. 1 Configuration of the proposed ubiquitous antenna system.

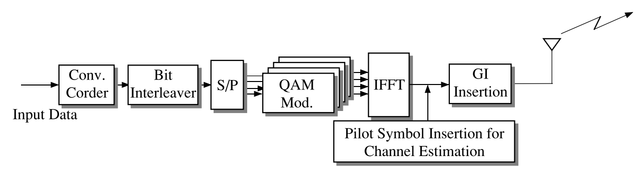

Fig. 2 Configuration of each mobile terminal.

CCS and RoF link. All the RBSs are deployed over the service area and connected to the CCS with RoF link. All the MTs in the service area transmit COFDM signals simultaneously at the same frequency channel. The transmitted co-channel signals interfere each other in radio propagation channel. They are also faded by multi-path Rayleigh fading and then received by some RBSs. The received RF signals at each RBS are converted to the optical signals by E/O converter and sent to the CCS via RoF link. The optical signals collected from multiple RBSs are converted to electrical signal again by O/E converters in the CCS. The CCS then performs a joint detection by the use of these signals, which keep their original RF signal formants, in order to receive the multi-user signals transmitted at the same frequency channel. The joint detection discussed in this paper cancels the co-channel interference by the optimum combining based on the independence of channel response between each MT and each RBS. Farther description about the joint detection is appeared in Sect. 2.2. Hence, the proposed system can achieve the SDMA which allows multiple MTs to operate at the same frequency channel and, as a result, remarkably improve the system capacity in terms of total number of users.

2.2 System Model

Now let us explain the system model considered in this paper along the signal flow. In this paper, we only focus on uplink communication. In following, we assume that each of M MTs simultaneously transmits COFDM signal at the same frequency channel, and L RBSs receive them.

Figure 2 shows the configuration of a COFDM transmitter equipped at each MT. We assume that all the MTs are uniformly deployed over the service area. The input data stream of m-th user is firstly convolutional encoded for forward error correction (FEC). The coded data stream is interleaved and mapped onto 2^k-quadrature amplitude modulation (QAM) symbols in subcarrier-by-subcarrier basis. The modulated subcarriers are then multiplexed at inverse fast Fourier transform (IFFT) processor. Pilot symbol for channel estimation and a guard interval, also known as the cyclic extension, are inserted. COFDM signal is finally transmitted to L RBSs dispersedly deployed in the cover area through radio propagation path.

In the radio propagation path, the signals transmitted from M co-channel MTs interfere each other and are faded by multi-path Rayleigh fading. The signals are received by L RBSs. The received signals are corrupted by the additive white Gaussian noise (AWGN) at the front end of each RBS. We call it radio link noise. For notational convenience, we define the $L \times 1$ received signals vector $\mathbf{y} = [y_1, y_2, \cdots, y_L]^T$ as

$$\mathbf{y} = \mathbf{H}\mathbf{x} + \mathbf{z}_r, \tag{1}$$

where the $M \times 1$ vector, $\mathbf{x}$, of transmitted signals and the $L \times 1$ radio link AWGN vector, $\mathbf{z}_r$, with zero mean and variance, σ_{nr}^2, are respectively given by

$$\mathbf{x} = [x_1, x_2, \cdots, x_M]^T, \tag{2}$$

$$\mathbf{z}_r = [z_{r1}, z_{r2}, \cdots, z_{rL}]^T, \tag{3}$$

where $\mathbf{x}^T$ denotes the transpose of $\mathbf{x}$. The frequency response matrix $\mathbf{H}$ of dimension $L \times M$ represents the radio link frequency response, which is constituted by the set of $L \times 1$ frequency response vectors of the M MTs,

$$\mathbf{H} = (\mathbf{H}_1, \mathbf{H}_2, \cdots, \mathbf{H}_M), \tag{4}$$

where $\mathbf{H}_m$ is given by

$$\mathbf{H}_m = [H_{m1}, H_{m2}, \cdots, H_{mL}]^T, \tag{5}$$

where H_{ml} is the frequency response between m-th MT and l-th RBS at the corresponding symbol and subcarrier. In this paper, we assume that H_{ml}'s are mutually independent, stationary, and complex Gaussian random variable with zero mean for different m's of l's.

At a RBS, the received radio signals are converted into the optical intensity modulated signal by an E/O converter, and sent to the CCS via the RoF link with their original RF signal formats kept. During the RoF link transmission, the noises generated in various sources corrupt the optical intensity modulated signals as shown in Fig. 3. The optical link noise power generally depends on the input signal power of E/O converter. In the ubiquitous antenna system, each RBS receives a different power signal from an MT since the distance between RBSs is about one hundred meters. However, multiple MTs transmit the signals at a same

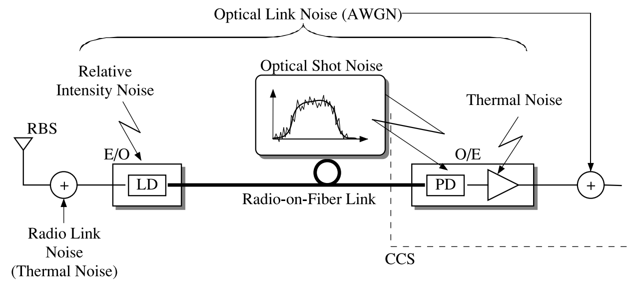

Fig. 3 The optical link noises considered in this paper.

frequency channel from different locations in the service area, and each RBS received them at the same time. Hence, we can consider the statistically mean value of received power at each RBS is approximately equal. In following, we express the optical link SNR as mean value, nominal E_b/N_0, in this paper, but an instantaneous SNR varies according to an instantaneous received signal power at each RBS.

The relative intensity noise (RIN) is generated at a laser diode when signals are applied to the E/O converter. The RIN is mainly due to amplified spontaneous emission and relaxation oscillation. Furthermore the non-linear distortion known as inter modulation distortion (IMD) caused by the laser diode nonlinearity is also generated at an E/O converter. In single octave multi-carrier transmission, inter modulation distortion, particularly third-order inter modulation distortion (IM3), have a great influence on RF signal quality as interferences. However, the RoF link is usually designed to obtain lower than -40 dBc of target IM3 power and, as a result, IM3 level could be less than other AWGN-type noise level [20]. Furthermore, the system can transmit OFDM signals via RoF link with keeping their orthogonality [21]. Hence, in following, we ignore the influence of IMD and consider only AWGN-type noise generated at optical link. At O/E converter in the CCS, moreover, the optical shot noise and the receiver thermal noise are generated due to photo detector and receiver circuits, respectively.

Furthermore, since the spacing amongst RBSs is around one hundred meters, about several hundreds nano seconds of delay difference has arisen in the RoF link. In general, this delay difference could be a serious problem in wideband transmission. Fortunately, since the COFDM signal has a guard interval inserted at the head of each COFDM symbol in order to avoid inter-symbol and inter-channel interference due to delay spread. We have previously shown that the delay difference can be tolerable when the distance between any two RBSs is shorter than 150 m [17]. Therefore, we need not consider the delay difference when indoor applications, such as wireless LAN, are assumed.

The CCS performs then the joint detection. Figure 4 shows the configuration of the CCS. The reconverted electrical signals are given by

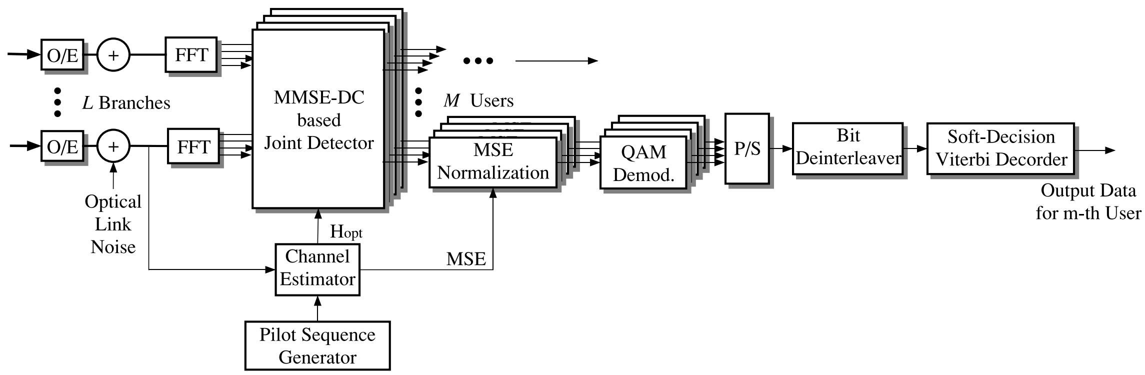

Fig. 4 Configuration of the central control station.

$$\mathbf{y} = G(\mathbf{H}\mathbf{x} + \mathbf{z}_r) + \mathbf{z}_o, \tag{6}$$

where $\mathbf{z}_o$ is $L \times 1$ optical link AWGN vector, zero mean and variance σ_{no}^2 and G means optical link gain.

Before joint detection, the received signals from L RBSs are divided into each subcarrier by the corresponding FFT processor. Then, the joint detection is performed in subcarrier-by-subcarrier basis. In this paper, we employ simple MMSE-DC as a joint detector. The MMSE-DC is one of the optimum diversity combiners which suppress the co-channel interference signals under the noise level. As a result, it can maximize the received SINR after combining and minimize mean square error between the desired signal and the estimated signal.

The $M \times L$ MMSE optimum weight matrix $\mathbf{H}_{opt}$ is given by

$$\mathbf{H}_{opt} = \mathbf{H}^H \mathbf{R}_{yy}^{-1}, \tag{7}$$

where $\mathbf{R}_{yy}$ is $L \times L$ correlation matrix of $\mathbf{y}$ and defined by

$$\mathbf{R}_{yy} = E_c[\mathbf{y}\mathbf{y}^H] \tag{8}$$

where E_C and $\mathbf{y}^H$ denote the conditional expectation and the Hermitian transpose of $\mathbf{y}$, respectively. The output of the MMSE-DC is given by

$$\hat{\mathbf{x}} = \mathbf{H}_{opt}\mathbf{y}. \tag{9}$$

$\hat{\mathbf{x}}$ is the estimated transmitted signal vector.

The output signals of MMSE-DC are then normalized by MSE, that is the noise variance of the corresponding signal, in order to maintain the gain at soft-decision Viterbi decoding in multipath environments [17]. The MSE for m-th MT is given by

$$MSE_m = \sigma_d^2 - \mathbf{H}_m^H \mathbf{R}_{yy}^{-1} \mathbf{H}_m, \tag{10}$$

where σ_d is the desired signal power [22]. Then, the normalized signals are demodulated, deinterleaved and decoded by the soft-decision Viterbi decoder. Finally, we can obtain the desired user's bit stream.

3. Simulation Results

3.1 Simulation Configurations

In following, we evaluate the performance of the proposed ubiquitous antenna based wireless LAN system with considering optical link noise by computer simulations. The optical link SNR is generally determined by RoF link configuration, such as fiber length, optical signal power, characteristic of E/O and O/E converters, transmission bandwidth of optical fiber and so on. However, in following simulations, in order to simplify the evaluation of their influence on the performance of the joint detection in the ubiquitous antenna system, we introduce the optical link SNR in form of E_b/N_0 in our simulations.

The COFDM signal configurations used in our simulation are shown in Table 1. Parameters are based on 5 GHz wireless LAN standards but little modified. As a subcarrier modulation format, we assume quadrature phase shift keying (QPSK) with coherent detection. As propagation channel, equal gain two-ray Rayleigh fading channel is assumed. The interval between two rays is 150 ns. The path loss exponent is 3.1, assumed for 5.2 GHz band operation in office environment [23]. We also assume that the symbol timing of the COFDM signals is synchronized at every MT. We ignore the frequency offset between MTs and CCS local oscillators.

The frequency response of the wireless channel between each MT and each RBS has to be precisely estimated to perform the MMSE-DC based joint detection. So, we attach the pilot symbols to the beginning of the packet which is composed of ten COFDM symbols. As unique word included in each MT's pilot symbol, we employ optimum MSE sequence discussed in [24], [25]. The CCS estimates the channel frequency response by calculating the correlation between received pilot symbols and the reference unique sequences. Furthermore, the initial phase for coherent detection can be also estimated by these pilot symbols.

The allocation of the RBSs in the service area is

Table 1 Simulation configurations.

Number of MTs and RBSs	4, 4
Modulation	QPSK-OFDM
FFT Size	64
Number of Subcarriers	48
Symbol Duration	4.2 μs
Guard Interval	1 μs
FEC	Convolution Constraint Length=7 Code Rate=1/2
Bit Rate	11.5 Mbits/s
Channel	Equal Gain 2-ray Rayleigh Fading Channel
RoF Link Delay	500 ns at Cell Size of 100 m
Path Loss Exponent	3.1

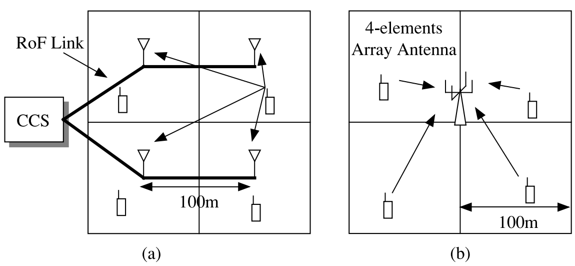

Fig. 5 The allocation of the RBSs for computer simulations. (a) Ubiquitous Antenna System (b) Central Antenna System.

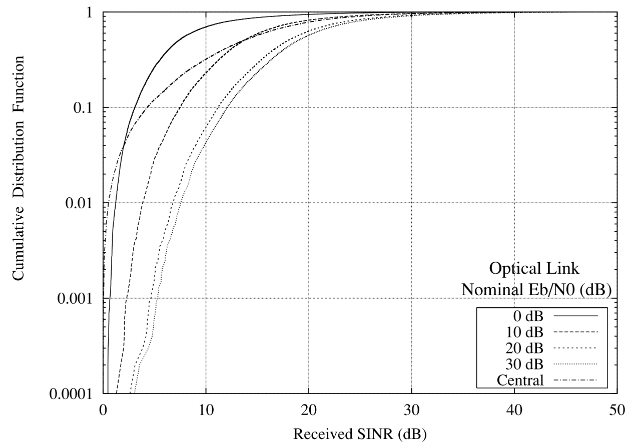

Fig. 6 Cumulative distribution of received SINR after combining at 15 dB of radio link nominal E_b/N_0.

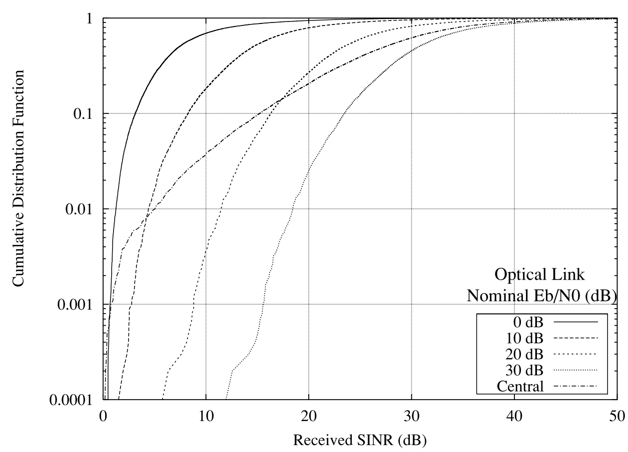

Fig. 7 Cumulative distribution of received SINR after combining at 30 dB of radio link nominal E_b/N_0.

shown in Fig. 5. We assume four RBSs case. In the ubiquitous antenna system as shown in Fig. 5(a) the service area is divided into four cells and one RBS is located at the center of each cell. The distance between any two RBSs is assumed to be 100 m. The RoF link connects all the RBSs to the CCS, which performs the MMSE-DC based joint detection. For comparison, we also evaluate the macro-cell system, where one RBS is located at the center of the service area as shown in Fig. 5(b). In the following, we call it the central antenna system. We assume that the central antenna system also performs joint detection with 4-elements array antenna and MMSE-DC based joint detection.

In this simulation, 4 MTs are uniformly distributed over the service area and simultaneously transmit COFDM signal at the same frequency channel in both system. In this simulation, we assume that the data rate is 11.5 Mbits/s at an occupied frequency bandwidth of 15 MHz. The transmission power of a MT is determined as nominal E_b/N_0, it is defined as the received E_b/N_0 when an RBS antenna receive the signal from the MT which is 70 m apart from it.

3.2 Evaluations of Received SINR

In the ubiquitous and central antenna systems, the received SINRs are varied depending on not only fading but also locations of MTs, it is one of the factor determining the level of path loss, if all the MTs transmit signals in the same transmission power. Furthermore, the locations of receive antennas in the ubiquitous antenna system are different from central one. Hence, it seems the variance of received SINR is also different in both systems. In order to investigate such differences, we firstly evaluate the received SINR after the joint detection and compare it with the central antenna system.

The received SINR after combining for m-th MT, γ_m, is given by

$$\gamma_m = \frac{\sigma_d^2}{\sigma_d^2 - \mathbf{H}_m^H \mathbf{R}_{yy}^{-1} \mathbf{H}_m}. \tag{11}$$

The dominator of Eq. (11) is MSE_m defined as Eq. (10) which includes noise components and the residual co-channel interference component after MMSE-DC.

Figures 6 and 7 show the cumulative distribution function of the received SINR in the ubiquitous and central antenna systems at 15 dB and 30 dB of radio link nominal E_b/N_0, respectively. In both figures, the vertical axis means cumulative distribution function of received SINR obtained from the 10,000 times trial runs about the locations of MTs which are given randomly in accordance with uniform distribution. From Figs. 6 and 7, we can find that the ubiquitous antenna system can cancel the co-channel interference because of the effect of the MMSE-DC based joint detection which maximize received SINR even if the optical link noise corrupts the signal. The probability that achieves high SINR becomes better as increasing radio and optical link nominal E_b/N_0.

Furthermore, we can also find that the differences between ubiquitous and central antenna systems. For example, from Fig. 7, the probability that the SINR is below 10 dB is lower than 0.01% when optical link nominal E_b/N_0 is 30 dB in the ubiquitous antenna system. On the other hand, in the central antenna system, the low SINR situations, lower than 10 dB, sometimes occur in spite of obtaining 30 dB of radio link nominal E_b/N_0. Hence, the ubiquitous antenna system can provide certain level of SINR over the service area. That is, the signal power is decentralized over the service area and each RBS receives a different power signal from the corresponding MT, which may be very different in level compared with the central antenna system. So that, since the gain of the joint detection is greater than that of the central antenna system, the ubiquitous antenna system provides above power gain.

3.3 Frequency Utilization Efficiency Performance

Next, we evaluate the frequency utilization efficiency of the proposed system. We assume that the transmission is successful when there is no bit error in a packet composed of one pilot symbol and ten information data symbols, and the maximum frequency utilization efficiency is 0.77 bits/s/Hz.

Figure 8 shows the frequency utilization efficiency against radio link nominal E_b/N_0. In this figure, the curve "conventional" shows the efficiency of the conventional system where 4 MTs transmit their COFDM signals at the same frequency channel with 4 time slots time division multiple access (TDMA) method, and its efficiency becomes low, up to 0.2 bits/s/Hz. The central antenna system achieves much higher efficiency than conventional system. On the other hand, the efficiency of the proposed ubiquitous antenna system depends on optical link E_b/N_0. The efficiency is lower than conventional system when optical link E_b/N_0 is 0 dB and radio link E_b/N_0 is more than 10 dB. However, the proposed ubiquitous antenna system achieves the same or higher efficiency than central antenna system when more than 20 dB of optical link E_b/N_0 is obtained. For example, about 0.7 bits/s/Hz can be achieved at 20 dB of radio link nominal E_b/N_0.

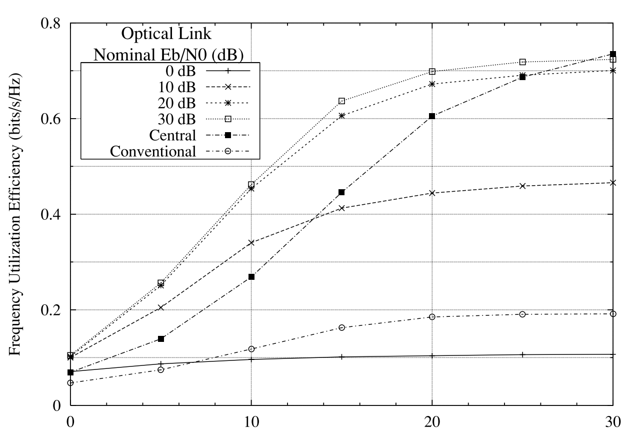

Fig. 8 The frequency utilization efficiency against radio link nominal E_b/N_0.

By the way, the received signal power of the desired MT at a RBS are generally different from the other RBSs since RBSs are dispersedly deployed in the ubiquitous antenna system. For example, the RBS near the corresponding MT obtains higher received signal power, on the other hand, the RBS far from it obtains lower. Such received power differences could be a problem when the CCS performs the joint detection. That is, the MMSE weight parameter defined as Eq. (7) is estimated from received signals as described in Sect. 3.1. Hence, the noise components included in the received signals cause parameter estimation errors. The MMSE-DC is no longer optimum and the performance is degraded when the error is large.

In order to avoid such a performance degradation, we consider the joint detection which does not use signal corrupted by noise components. So, we also evaluate the performance of the joint detection which uses one or two or three RBS signals, not all four RBSs, in the order of descending received signal power. The received signal power level could be estimated from channel response. The simulation results is shown in Fig. 9. Figure 9 shows the number of RBSs used in the joint detection which provides the best frequency utilization efficiency in the simulations run with varying the number of RBSs from one to four against radio and optical link nominal E_b/N_0. The horizontal and vertical axes show radio and optical link nominal E_b/N_0, respectively. In Fig. 9, The joint detection using only one RBS signal which obtains the largest signal power provides better frequency utilization efficiency than that using all four RBSs when radio and/or optical link nominal E_b/N_0 is less than 4 dB. On the other hand, the joint detection using all four RBSs provides the best performance when the system obtains 12 dB and 14 dB of radio and optical link nominal E_b/N_0, respectively, since the noise components included in the MMSE weight parameter are negligible. Hence, from Fig. 9, we can find that the system could improve the frequency utilization efficiency by the selecting the number of using RBSs according to radio and optical link nominal E_b/N_0, and it is more important to avoid the MMSE parameter estimation error than to obtain the diversity gain in low radio and/or

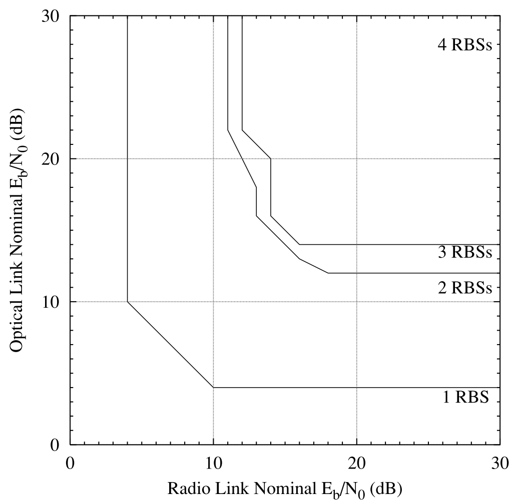

Fig. 9 The number of the combining RBSs which provides the best frequency utilization efficiency in the simulations run with varying the number of the combining RBSs from one to four against radio and optical link nominal E_b/N_0.

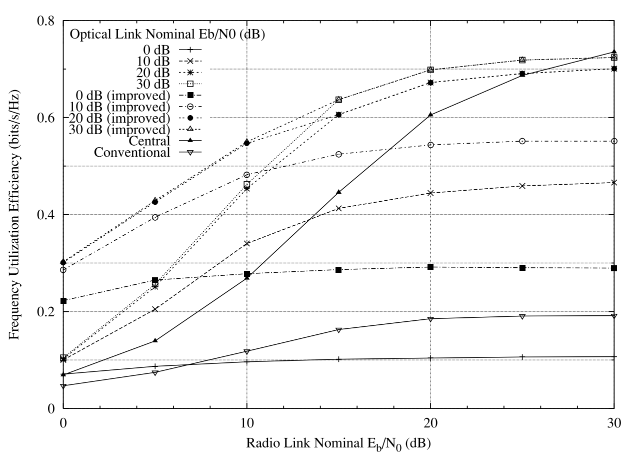

Fig. 10 The frequency utilization efficiency of the ubiquitous antenna system with the joint detection using variable number of RBS signals. (The cases of central, central and ubiquitous with the joint detection using all four RBSs are also shown.)

optical link nominal E_b/N_0 cases.

Figure 10 shows the frequency utilization efficiency of the ubiquitous antenna system with the joint detection using variable number of RBS signals. In this paper, we have not proposed the algorithm which decide the number of RBSs adaptively. Hence, the system varies the number of RBSs according to nominal E_b/N_0 shown in Fig. 9. For comparison purposes, the frequency utilization efficiency of the ubiquitous antenna system with joint detection using all four RBSs, central and conventional one are also shown in Fig. 10. From Fig. 10, there is no difference in the frequency utilization efficiency between both ubiquitous antenna systems in the case of more than 15 dB and 20 dB of radio and optical link nominal E_b/N_0 case, respectively, since both system perform joint detection using all four

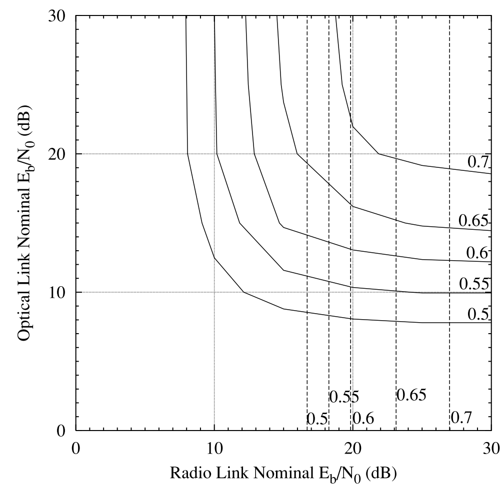

Fig. 11 The frequency utilization efficiency contours; plane: the ubiquitous antenna system, dashed: the central antenna system.

RBSs. The system, on the other hand, can improve the frequency utilization efficiency by selecting appropriate number of RBSs according to radio and optical link E_b/N_0 in lower radio and optical link E_b/N_0 cases because of the avoidance of MMSE parameter estimation errors. Especially, approximately twice efficiency is obtained in 0 dB of radio and/or optical link nominal E_b/N_0 cases.

Finally, we show the frequency utilization efficiency contours of the ubiquitous and central antenna systems in Fig. 11. In Fig. 11, horizontal and vertical axes show radio and optical link nominal E_b/N_0, respectively. In case of the central antenna system (represented by dashed line), the system requires more than 27 dB radio link nominal E_b/N_0 for achieving 0.7 bits/s/Hz efficiency. In the ubiquitous antenna system, on the other hand, the efficiency varies depending on optical link nominal E_b/N_0 even if radio link nominal E_b/N_0 is constant. When the optical link is assumed to be ideal, the asymptotic line of contour for the efficiency of 0.7 bits/s/Hz shows that the required radio link E_b/N_0 is about 19 dB. Therefore, the ubiquitous antenna system obtain about 8 dB of radio link power gain compared with the central antenna system when the optical link noise is negligible. This radio link power gain results from distributed installation of RBSs same as the received SINR characteristic as shown in Figs. 6 and 7. However, the gain decreases with decreasing optical link E_b/N_0 when the optical link noises are considered. From Fig. 11, we can find that the required optical link E_b/N_0 for achieving 0.7 bits/s/Hz efficiency is 19 dB under condition of the same radio link E_b/N_0 as the central antenna system. Hence, if we maintain the RoF link configurations of the ubiquitous antenna system to obtain more than 19 dB of optical link E_b/N_0, the ubiquitous antenna system obtains maximum of 8 dB of radio link power gain compared with central antenna system because of its distributed installation of RBSs. Moreover, the region where the efficiency is higher than 0.7 bits/s/Hz of the ubiquitous antenna system is wider than that of the central antenna system. Furthermore, since it is previously shown that the system usually obtain 40 dB of optical link signal-to-noise ratio (SNR) [12], the ubiquitous antenna system can satisfy above condition.

4. Conclusions

In this paper, we have introduced the ubiquitous antenna system which improves the frequency utilization and power efficiency of the broadband wireless LAN system and investigated its performance with consideration of the optical link noise by computer simulations.

Form the computer simulation results, we have found the following improvement;

- The proposed ubiquitous antenna system can provide certain level of SINR over the service area.
- The proposed system can achieve higher efficiency than the other systems when more than 20 dB of optical link nominal E_b/N_0 is obtained.
- The proposed system provides 8 dB of radio link power gain compared with central array antenna system.
- The region where the efficiency is higher than 0.7 bits/s/Hz of the ubiquitous antenna system is wider than that of the central antenna system although the optical link noise causes the degradation of the performance of the system.
- We have to maintain the RoF link configurations to obtain more than 19 dB of optical link E_b/N_0.

However, we have considered only AWGN-type noise generated in optical link in this paper. To develop more extensional discussion, we will have to strictly consider the influence of the non-linear distortion and properties of optical devices on the performance of the proposed system as further studies.

Acknowledgement

This paper is partially supported by the Grants-in-Aid for Scientific Research (B) No. 143502002, form the Japan Society for the Promotion of Science.

References

[1] R. van Nee, G. Awater, M. Morikura, H. Takanashi, M. Webster, and K.W. Halford, "New high-rate wireless LAN standards," IEEE Commun. Mag., vol.37, no.12, pp.82–88, Dec. 1999.

[2] M. Morikura and H. Matsue, "Trends of IEEE 802.11 based wireless LAN," IEICE Trans. Commun. (Japanese Edition), vol.J84-B, no.11, pp.1918–1927, Nov. 2001.

[3] R.D. Murch and K.B. Letaief, "Antenna system for broadband wireless access," IEEE Commun. Mag., vol.40, no.4, pp.76–83, April 2002.

[4] V. Tarokh, H. Jafarkhani, and A.R. Calderbank, "Space-time block coding for wireless communications: Performance results," IEEE J. Sel. Areas Commun., vol.17, no.3, pp.451–460, March 1999.

[5] Y. Li, J.C. Chuang, and N.R. Sollenberger, "Transmitter diversity for OFDM systems and its impact on high-rate data wireless networks," IEEE J. Sel. Areas Commun., vol.17, no.7, pp.1233–1243, July 1999.

[6] L. Giangaspero and G. Paltenghi, "A MIMO architecture for wireless indoor applications," Proc. IEEE ICWLHN 2001, pp.317–326, Dec. 2001.

[7] S. Hori, M. Mizoguchi, T. Sakata, and M. Morikura, "A new branch metric generation method for soft-decision Viterbi decoding in coded OFDM-SDM systems employing MLD over frequency selective MIMO channels," IEICE Trans. Fundamentals, vol.E85-A, no.7, pp.1675–1684, July 2002.

[8] H. Al-Raweshidy and S. Komaki, Radio over Fiber Technologies for Mobile Communications Network, pp.82–94, pp.183–216, pp.241–248, Artech House Publishers, 2002.

[9] S. Komaki, K. Tsukamoto, M. Okada, and H. Harada, "Proposal of radio highway networks for future multimedia-personal wireless communications," ICPWC'94, pp.204–208, Bangalore, India, Aug. 1994.

[10] S. Okamura, M. Okada, K. Tsukamoto, and S. Komaki, "Throughput improvement to CSMA/CA packetized wireless access system based on ubiquitous antennas," IEICE Technical Report, RCS2002-150, Aug. 2002.

[11] Y. Park, S. Miyamoto, S. Komaki, and N. Morinaga, "The effect of co-channel interferences on intercell diversity in the optical microcell system," IEICE Technical Report, SAT93-62, RCS93-68, Oct. 1993.

[12] T. Okada, M. Okada, and S. Komaki, "Control free intercell diversity using multi-carrier modulation for fiber-optic microcellular radio communication system," Proc. IEEE ICUPC'95, pp.486–490, Nov. 1995.

[13] Y.H. Park, M. Okada, and S. Komaki, "The performance of fiber-radio road vehicle communication system with macro-diversity," Wireless Personal Communications, vol.14, pp.125–132, 2000.

[14] M. Toyama, M. Okada, and S. Komaki, "Maximal ratio combining macro diversity for micro-cellular slotted ALOHA," IEICE Trans. Commun. (Japanese Edition), vol.J79-B-I, no.5, pp.271–277, May 1996.

[15] S. Okamura, M. Okada, and S. Komaki, "Impact of ubiquitous antennas to the interference cancellation of COFDM systems," Proc. 6th International OFDM-Workshop (InOWo'01), 2-1, Sept. 2001.

[16] S. Okamura, M. Okada, and S. Komaki, "Improvement of frequency utilization efficiency based on ubiquitous antennas," IEICE Technical Report, MoMuC 2001-39, Nov. 2001.

[17] S. Okamura, M. Okada, and S. Komaki, "Ubiquitous antenna system for joint detection of COFDM signals," IEICE Trans. Fundamentals, vol.E85-A, no.7, pp.1685–1692, July 2002.

[18] Y. Li and R. Sollenberger, "Adaptive antenna arrays for OFDM systems with cochannel interference," IEEE Trans. Commun., vol.47, no.2, pp.217–229, Feb. 1999.

[19] S. Okamura, M. Okada, K. Tsukamoto, and S. Komaki, "Impact of optical link noise on the performance of ubiquitous antenna system," Proc. 2002 Asia-Pacific Microwave Conference, vol.1, pp.103–106, Nov. 2002.

[20] T. Niiho, H. Sasai, K. Masuda, and S. Morikura, "Radio-on-fiber link using direct modulation in 5-GHz band," Proc. 2002 International Topical Meeting on Microwave Photonics, W3-2, pp.25–28, Nov. 2002.

[21] R. Watanabe, Y. Horiuchi, H. Tanaka, and M. Suzuki, "Optical modulation characteristics of 5.8 GHz OFDM sig-

nal with electro-absorption modulator," Proc. 2002 International Topical Meeting on Microwave Photonics, P3-3, pp.221–224, Nov. 2002.
[22] S. Haykins, Adaptive Filter Theory 3rd Edition, Prentice-Hall, 1996.
[23] Rec. ITU-R P.1238-1, "Propagation data and prediction methods for the planning of indoor radiocommunication systems and radio local area networks in the frequency range 900 MHz to 100 GHz," 1999.
[24] Y. Li, N. Seshadri, and S. Ariyavisitakul, "Channel estimation for OFDM systems with transmitter diversity in mobile wireless channels," IEEE J. Sel. Areas Commun., vol.17, no.3, pp.461–471, March 1999.
[25] M. Mümster and L. Hanzo, "Improved decision-directed channel estimation for multi-user OFDM environments," Proc. Vehicular Technology Conference, Rhodes, Greece, IEEE, May 2001.

Shutai Okamura was born in Muroto, Japan, in 1977. He received the B.E. degree in electrical and electronic engineering from Shizuoka University, in 2000, and the M.E. degree in Communications Engineering from Osaka University, in 2001. He is currently pursuing the Ph.D. degree at Osaka University, and engaging in the research on radio communication systems. He is a member of IEEE.

Minoru Okada received the B.E. degree in communications engineering from the University of Electro-Communications, Tokyo, Japan, in 1990 and the M.E. and Ph.D. degrees both in communications engineering from Osaka University, Osaka, Japan, in 1992 and 1998, respectively. Since 1993, he was with the Department of Communications Engineering, Osaka University, as a Research Associate. From 1999 to 2000, he was with the University of Southampton, U.K., as a Visiting Research Fellow. In 2000, he joined the Graduate School of Information Science, Nara Institute of Science and Technology, Nara, Japan, where he is currently an Associate Professor. Dr. Okada is a member of the Institute of Electrical and Electronics Engineers (IEEE), and the Institute of Image Information and Television Engineers of Japan (ITE). He received the Young Engineer Award from IEICE in 1999.

Katsutoshi Tsukamoto was born in Shiga, Japan in October 7, 1959. He received the B.E., M.E. and Ph.D. degrees in Communications Engineering from Osaka University, in 1982, 1984 and 1995 respectively. He is currently an Associate Professor in the Department of Communications Engineering at Osaka university, engaging in the research on radio optical communication systems. He is a member of IEEE and ITE. He was awarded the Paper Award of IEICE, Japan in 1996.

Shozo Komaki was born in Osaka, Japan in 1947. He received the B.E., M.E. and Ph.D. degrees in Communications Engineering from Osaka University, in 1970, 1972 and 1983 respectively. In 1972, he joined the NTT Radio Communication Labs., where he has engaged in repeater development for a 20-GHz digital radio system, 16-QAM and 256-QAM systems. From 1990, he moved to Osaka University, Faculty of Engineering, and engaging in the research on radio and optical communication systems. He is currently a Professor of Osaka University. Dr. Komaki is a senior member of the Institute of Television Engineering of Japan (ITE). He was awarded the Paper Award and the Achievement Award of IEICE, Japan in 1977 and 1994 respectively.